

# Mitochondrial Nitroreductase Activity Enables Selective Imaging and Therapeutic Targeting

Arnaud Chevalier, Yanmin Zhang, Omar M. Khdour, Justin B. Kaye, and Sidney M. Hecht\*

Biodesign Center for BioEnergetics, and School of Molecular Sciences, Arizona State University, Tempe, Arizona 85287, United States

## Supporting Information

**ABSTRACT:** Nitroreductase (NTR) activities have been known for decades, studied extensively in bacteria and also in systems as diverse as yeast, trypanosomes, and hypoxic tumors. The putative bacterial origin of mitochondria prompted us to explore the possible existence of NTR activity within this organelle and to probe its behavior in a cellular context. Presently, by using a profluorescent near-infrared (NIR) dye, we characterize the nature of NTR activity localized in mammalian cell mitochondria. Further, we demonstrate that this mitochondrially localized enzymatic activity can be exploited both for selective NIR imaging of mitochondria and for mitochondrial targeting by activating a mitochondrial poison specifically within that organelle. This constitutes a new mechanism for mitochondrial imaging and targeting. These findings represent the first use of mitochondrial enzyme activity to unmask agents for mitochondrial fluorescent imaging and therapy, which may prove to be more broadly applicable.

Recent publications have described the potential importance of mitochondrial targeting for the development of new therapeutic agents such as anticancer agents.<sup>1</sup> For example, selective induction of elevated reactive oxygen species levels in mitochondria has been found to produce different effects in cancer cells than in normal cells.<sup>1</sup> Several types of agents that affect mitochondrial function have been the focus of preclinical studies,<sup>2</sup> which argues for the relevance of this strategy. While mitochondrial localization has been reported for numerous molecules,<sup>3</sup> notably those containing a lipophilic cation,<sup>4</sup> incorporating a mitochondrial targeting moiety within a molecule may prove challenging in the broader context of molecular design for a specific cellular target.

An alternative strategy might involve the organelle-specific enzymatic activation of an inactive prodrug,<sup>5</sup> e.g., by an enzymatic activity abundant within the organelle.<sup>6</sup> The generally accepted bacterial origin of mitochondria<sup>7</sup> led us to investigate bacterial enzymatic activities of potential utility for mitochondrial prodrug activation. The presence of redox enzymes in bacteria is now well established,<sup>8</sup> and bacterial nitroreductase (NTR) has been reported to reduce nitroaryl compounds to the corresponding (hydroxy)anilines by one of two mechanisms.<sup>9</sup> One of these, type I NTR, involves an initial two-electron reduction of nitro groups and is tolerant of oxygen, permitting nitro group reduction to proceed to completion (Figure 1a). Type II NTR, in contrast, involves an initial one-electron reduction and proceeds to

completion only under hypoxic conditions.<sup>9</sup> While NTR activity in human cells appears to have been reported thus far only in hypoxic tumors,<sup>10</sup> early reports of NTR activity in mitochondrial fractions isolated from mammalian liver cells<sup>11</sup> suggested the possible existence of type I mitochondrial NTR activity.

Detection of NTR activities within hypoxic tumor tissue using fluorogenic methods has been described recently, as reviewed by Elmes,<sup>12</sup> presumably involving type II NTR(s). Fluorescent probes have also been designed to measure small chemical species within mitochondria.<sup>4,13</sup> In comparison, there appears to have been no enzymatic activity detected in mitochondria using a fluorogenic method.

In an effort to detect a mitochondrial NTR which could be used for mitochondrial imaging, we designed a positively charged<sup>6</sup> fluorogenic probe which could potentially be triggered by a NTR.<sup>14</sup> The QCy7 system<sup>15</sup> seemed to be a good candidate. It exhibits an emission wavelength in the NIR region which affords good cell imaging efficiency by diminishing the background and enhancing light penetrability. Also, the presence of indoles permitted the introduction of positive charge by simple indole alkylation (Scheme 1). Preparation of *ortho*-, *meta*-, and *para*-substituted 4-nitrobenzyloxy-isophthalaldehydes provided the alkylated precursors **1a–1c** required for synthesis of the protected QCy7 dyes. The dialdehydes were used to prepare three new probes by treatment with an excess of 1-ethyl-2,3,3-trimethyl-3H-indolium iodide (pyridine and/or Ac<sub>2</sub>O, 80 °C, 3 h) as outlined in Scheme 1.

The proposed strategy for release of the fluorescent NIR dye from a nonfluorescent precursor via mitochondrial NTR-mediated reduction involved successive reduction and then elimination (Figure 1b). The use of *ortho*-, *meta*-, and *para*-substituted probes **2a–2c** was crucial because it enabled us to investigate the proposed transformation in greater detail. Even if reductive elimination of the *ortho*- and *para*-substituted probes proved to be practicable, none should occur in the case of *meta*-substituted analogue **2b**. To assess the viability of these probes for the detection of NTR activity, we first validated the probes in a cell-free system using purified *E. coli* NTR. Probes **2a–2c** (10 μM) were incubated in PBS buffer, pH 7.4, containing 0.5 mM NADH. After a short time, during which no fluorescence was observed, NTR was added (1 μg/mL), and the development of fluorescence was monitored as a function of time (Figure 2a,b). As expected, no fluorescence increase was observed for the probe **2b** (*meta*-substituted). The use of a greater (5 μg/mL) concentration of

Received: June 16, 2016

Published: August 29, 2016

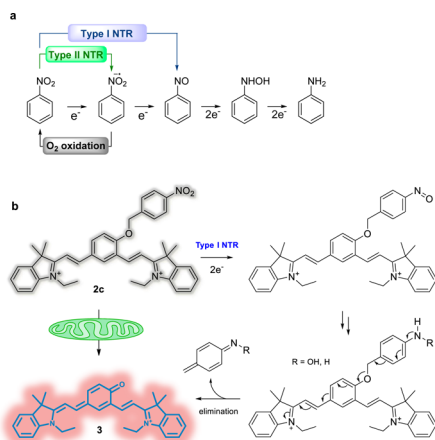


**Figure 1.** Plausible mechanism of nitroreductase (NTR) activation of fluorophore 3. (a) General mechanisms proposed<sup>9</sup> for type I and type II NTRs. (b) Mechanism of type I NTR reduction applied to the activation of probe 2c.

### Scheme 1. Synthesis of NTR-Activatable Profluorescent Probes 2a–2c

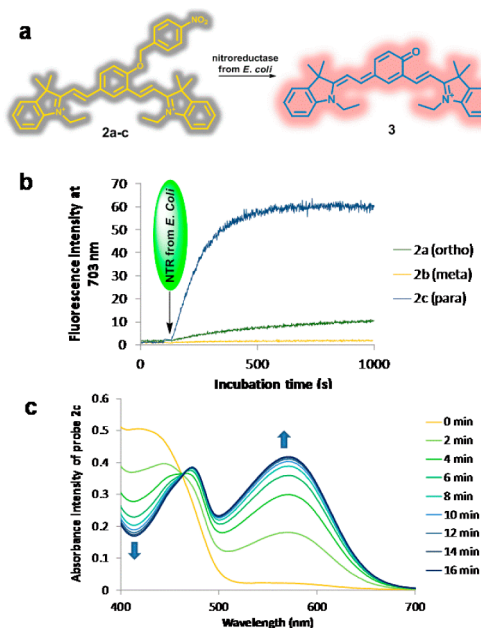
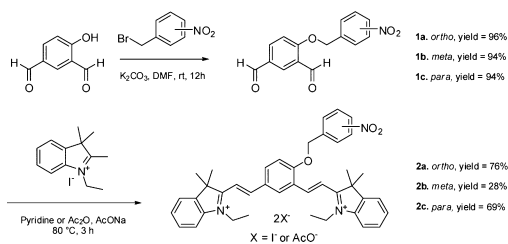


**Figure 2.** (a) Selective activation of 2c *in vitro* by *E. coli* NTR. (b) Time-dependent fluorescence emission by 2a, 2b, and 2c (excitation at 572 nm; emission at 703 nm) in PBS at 25 °C following treatment with *E. coli* NTR (1 μg/mL) and 0.5 mM NADH. (c) Absorbance spectrum evolution with time during incubation of probe 2c in 25 μM PBS buffer, pH 7.4, with *E. coli* NTR (1 μg/mL) and 0.5 mM NADH.

NTR also failed to produce any detectable activation of 2b. Conversely, good activation was observed for 2a and 2c, which are

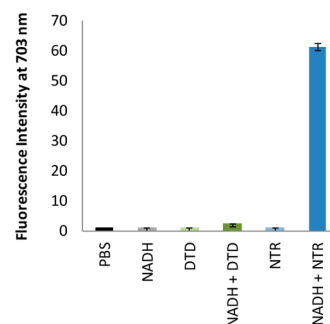


**Figure 3.** Development of fluorescence from 10 μM 2c following treatment with 1 μg/mL DT diaphorase (DTD) or nitroreductase (NTR) in 10 mM PBS buffer, pH 7.4, for 20 min at 25 °C with or without 0.5 mM NADH.

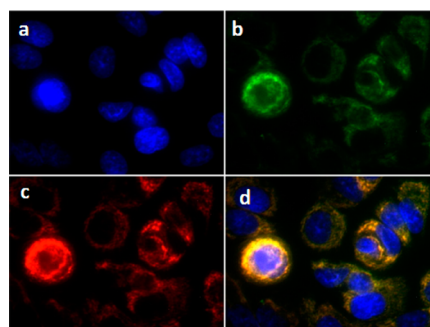


**Figure 4.** Fluorescence emission from 2c colocalized to mitochondria in live A549 cells. Cells were stained with (a) 2.5 μg/mL DAPI for nuclear staining, (b) 100 nM MitoTracker Green FM for mitochondrial staining, and (c) 10 μM 2c for NTR detection. (d) Overlay of images a–c.

*ortho*- and *para*-substituted, respectively. This confirmed our expectation but also revealed that activation of 2c was much faster than that of 2a and increased with increasing substrate concentration (Supporting Information (SI), Figures S1 and S2). This can be explained by a better binding of the *p*-nitrobenzyl compounds in the NTR enzyme active site, as reported recently by Li et al.<sup>10b</sup>

The selectivity of the probe was also investigated using DT diaphorase, another two-electron reductase capable of activating small molecules.<sup>16</sup> As shown in Figure 3, significant activation occurred only in the presence of NTR + NADH, also affirming the NADH dependency of the enzyme.<sup>17</sup> Monitoring the absorbance spectrum during NTR activation of 2c (Figure 2c) showed an increase of the absorbance band centered at 572 nm. This confirms that the released fluorescent dye is effectively of the QCy7 type by comparison with an authentic standard prepared by chemical synthesis (SI, Figure S3).

With the viability of this probe thus confirmed, we carried out microscopy experiments employing A549 cancer cells (Figure 4). Incubation of 10 μM 2c with the cells for 4 h was followed by addition of 100 nM MitoTracker Green (40 min incubation).

The results clearly show the appearance of a red signal (Figure 4c) characteristic of the release of QCy7 dye 3. The green channel (Figure 4b) illustrates visualization of the mitochondria by MitoTracker Green. Superposition of panels a–c (Figure 4d) shows complete overlap of the red and green signals, resulting in a yellow signal around the nucleus (stained in blue using DAPI). As a control, probes 2a and 2b were also tested and did not provide a good signal at 4 h (SI, Figure S4). This is understandable for 2b, as no elimination process is possible, as confirmed during the *in vitro*

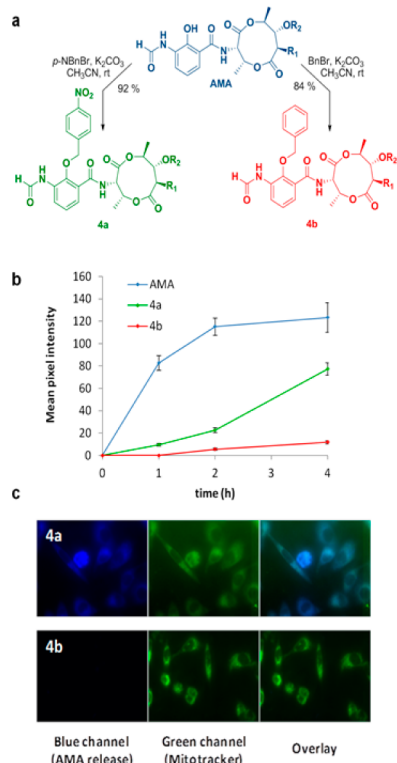


**Figure 5.** Use of NTR for antimycin A (AMA) release in mitochondria. (a) Syntheses of *p*-nitrobenzyl-*O*-AMA (**4a**) and benzyl-*O*-AMA (**4b**) through alkylation of AMA. (b) Time course of appearance of AMA fluorescence ( $\lambda_{em} \approx 425$  nm)<sup>18</sup> during microscopy experiments in live A549 cancer cells treated with AMA and its alkylated derivatives **4a** and **4b** at 25  $\mu$ M concentrations for 4 h. The need for high concentrations of **4a**/**4b** reflected the low quantum yield of the released AMA ( $\sim 0.06$ ). (c) AMA fluorescence signal after release by NTR from alkylated analogues of AMA. Free AMA appeared exclusively in the mitochondria following treatment with **4a**, while treatment with **4b** resulted in no significant release of AMA.

tests. In the case of **2a**, we assume that the low kinetics of the reduction (Figure 2b) is probably the cause of the absence of a strong signal. The appearance of a signal from **2c** was concentration dependent (SI, Figure S5), was weaker after shorter incubation times (SI, Figure S6), and was inhibited by the bacterial NTR inhibitor dicoumarol<sup>18</sup> (SI, Figure S7). We note that no fluorescence has been reported using NIR dyes not targeted to the mitochondria.<sup>12</sup> This constitutes the first direct visualization of NTR activity localized in mitochondria. Notably, no hypoxic condition was required, i.e., the observed activity must be of type I, but this does not exclude the possible additional presence of one or more type II NTRs in the mitochondria. The selectivity of this probe for mitochondrial NTR under normoxic conditions might well be exploitable for more accurate imaging of the mitochondria. In comparison with mitotracker imaging agents, which accumulate in the mitochondria by virtue of their positive charge and the polarization of the mitochondrial membrane, the present probe is profluorescent and converted to a fluorophore exclusively in the presence of NTR, i.e., within the mitochondria.

The finding of NTR activity associated with the mitochondria of human cells encouraged us to design a new prodrug based on the mitochondrial poison antimycin A (AMA). We recently noted that AMA is toxic only at relatively high concentration,<sup>19</sup> plausibly due to a lack of facile access to the mitochondria. Further, it has

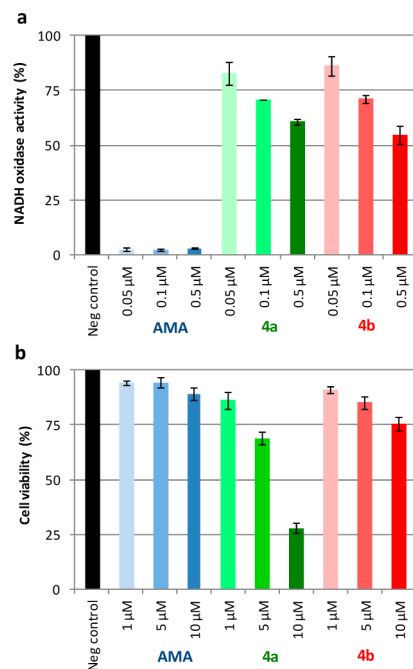


**Figure 6.** Biological activity of AMA, **4a**, and **4b**, (a) NADH oxidase activity assays on AMA, **4a**, and **4b** at 0.05, 0.1, and 0.5  $\mu$ M concentrations. (b) Cytotoxicity of AMA, **4a**, and **4b** toward A549 lung cancer cells after 24 h of incubation at 1, 5, and 10  $\mu$ M concentrations.

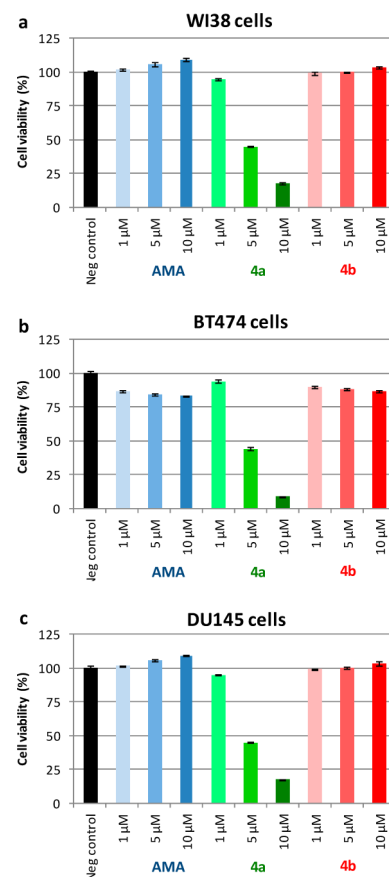


**Figure 7.** Cytotoxicity of AMA, **4a**, and **4b** toward (a) WI38 normal human lung cells, (b) BT474 breast cancer cells, and (c) DU145 prostate cancer cells after 24 h of incubation with these compounds at 1, 5, and 10  $\mu$ M concentrations.



been shown that there is at least one locus of action for AMA that does not involve the respiratory chain.<sup>20</sup> It seemed possible that, by *O*-alkylating AMA with a *p*-nitrobenzyl moiety, we might facilitate mitochondrial delivery and release the active form of the compound only in the mitochondria. Accordingly, *O*-*p*-nitrobenzyl-AMA (**4a**) was prepared in good yield by alkylation of AMA (Figure 5a). Also prepared as a negative control was *O*-benzyl-AMA (**4b**). Compounds **4a** and **4b** lack fluorescence, while AMA is fluorescent.<sup>18</sup> It should thus be possible to monitor the release of AMA within the mitochondria after enzymatic reduction of the nitro moiety in **4a**. As anticipated, AMA was released from **4a** by the action of mitochondrial NTR, but not to a significant extent from **4b** (Figure 5b), and its appearance was localized to the mitochondria (Figure 5c). In comparison, A549 cells treated with AMA resulted in a distribution of AMA which did not fully colocalize with mitochondria (SI, Figure S8).

Evaluation of **4a** and **4b** relative to AMA was carried out by comparing their effects both on the activity of the mitochondrial respiratory chain and on cell viability. As shown in Figure 6a, AMA was a potent inhibitor of NADH oxidase, which measures the activity of mitochondrial respiratory complexes I, III, and IV. While AMA inhibited NADH oxidase essentially completely at 50 nM concentration, **4a** and **4b** exhibited much weaker activity. This is not surprising, given the putative importance of the phenolic moiety in AMA in association with the respiratory chain through hydrogen bonding.<sup>21</sup> Despite their similar inhibitory activity toward NADH oxidase, **4a** was much more cytotoxic toward A549 cancer cells than **4b**, no doubt due to the conversion of **4a** to AMA within the mitochondria by the NTR. Compound **4a** was considerably more cytotoxic than exogenously added AMA despite the ready cellular uptake of AMA (Figure 5b), underscoring the belief that the latter is not delivered efficiently to the mitochondria. This represents the first example of the use of a mitochondrial NTR for selective mitochondrial drug delivery, and should be extensible to numerous other classes of potential therapeutic agents. We note that **4a** is not positively charged, so its mitochondrial delivery must be due to some other facet of its structure.<sup>3</sup>

To explore the generality of the biological phenomena noted above in other cell lines, we also studied the cytotoxic effects of AMA, **4a**, and **4b** on three other human cell lines. As noted in Figure 7, the effects of the compounds on these cell lines were closely analogous to what was observed for cultured A549 lung cancer cells. The experiments shown in Figures 6b and 7a were also carried out for 48 h with quite similar results (SI, Figure S9).

In summary, we have identified a type I nitroreductase within the mitochondria of A549 human lung adenocarcinoma cells and demonstrated that this activity could be employed for the selective mitochondrial release of a fluorescent QCy7 dye from a caged, non-fluorescent precursor that was transported into the mitochondria. The same protecting group was used to prepare a prodrug of the mitochondrial poison antimycin A. The prodrug was transported into the mitochondria more efficiently than AMA itself, leading to more potent cell killing. The AMA prodrug **4a** exhibited the same cytotoxic effects in comparison with AMA and prodrug **4b** in three additional human cell lines.

## ■ ASSOCIATED CONTENT

### 📄 Supporting Information

The Supporting Information is available free of charge on the ACS Publications website at DOI: 10.1021/jacs.6b06229.

Experimental details (PDF)

## ■ AUTHOR INFORMATION

### Corresponding Author

\*sid.hecht@asu.edu

### Notes

The authors declare no competing financial interest.

## ■ REFERENCES

- (1) (a) Wallace, D. C. *Nat. Rev. Cancer* **2012**, *12*, 685. (b) Sullivan, L. B.; Chandel, N. S. *Cancer Metab.* **2014**, *2* (1), 17. (c) Weinberg, S. E.; Chandel, N. S. *Nat. Chem. Biol.* **2015**, *11*, 9.
- (2) (a) Lessene, G.; Czabotar, P. E.; Colman, P. M. *Nat. Rev. Drug Discovery* **2008**, *7*, 989. (b) Kang, M. H.; Reynolds, C. P. *Clin. Cancer Res.* **2009**, *15*, 1126. (c) Yeh, C.-T.; Su, C.-L.; Huang, C.-Y. F.; Lin, J. K.-Y.; Lee, W.-H.; Chang, P. M.-H.; Kuo, Y.-L.; Liu, Y.-W.; Wang, L.-S.; Wu, C.-H.; Shieh, Y.-S.; Jan, Y.-H.; Chuang, Y.-J.; Hsiao, M.; Wu, A. T. H. *Evid.-Based Comp. Alt. Med.* **2013**, *2013*, 910451.
- (3) (a) Rin Jean, S.; Tulumello, D. V.; Wisnovsky, S. P.; Lei, E. K.; Pereira, M. P.; Kelley, S. O. *ACS Chem. Biol.* **2014**, *9*, 323. (b) Ma, J.; Lim, C.; Sacher, J. R.; Van Houten, B.; Qian, W.; Wipf, P. *Bioorg. Med. Chem. Lett.* **2015**, *25*, 4828.
- (4) Xu, Z.; Xu, L. *Chem. Commun.* **2016**, *52*, 1094.
- (5) Kratz, F.; Mueller, I. A.; Ryppa, C.; Warnecke, A. *ChemMedChem* **2008**, *3*, 20.
- (6) Clearly, it would also be possible to employ this strategy in conjunction with an organelle targeting strategy.
- (7) (a) Gray, M. W.; Burger, G.; Lang, B. F. *Science* **1999**, *283*, 1476. (b) Herrmann, J. M. *Trends Microbiol.* **2003**, *11*, 74.
- (8) Symons, Z. C.; Bruce, N. C. *Nat. Prod. Rep.* **2006**, *23*, 845.
- (9) Williams, E. M.; Little, R. F.; Mowday, A. M.; Rich, M. H.; Chan-Hyams, J. V. E.; Copp, J. N.; Smail, J. B.; Patterson, A. V.; Ackerley, D. F. *Biochem. J.* **2015**, *471*, 131.
- (10) (a) Cui, L.; Zhong, Y.; Zhu, W.; Xu, Y.; Du, Q.; Wang, X.; Qian, X.; Xiao, Y. *Org. Lett.* **2011**, *13*, 928. (b) Li, Y.; Sun, Y.; Li, J.; Su, Q.; Yuan, W.; Dai, Y.; Han, C.; Wang, Q.; Feng, W.; Li, F. *J. Am. Chem. Soc.* **2015**, *137*, 6407.
- (11) (a) Moreno, S. N. J.; Mason, R. P.; Docampo, R. J. *Biol. Chem.* **1984**, *259*, 6298. (b) Smyth, G. E.; Orsi, B. A. *Biochem. J.* **1989**, *257*, 859.
- (12) Elmes, R. B. P. *Chem. Commun.* **2016**, *52*, 8935.
- (13) (a) Dickinson, B. C.; Chang, C. J. *J. Am. Chem. Soc.* **2008**, *130*, 9638. (b) Dodani, S. C.; Leary, S. C.; Cobine, P. A.; Winge, D. R.; Chang, C. J. *J. Am. Chem. Soc.* **2011**, *133*, 8606. (c) Kong, X.; Su, F.; Zhang, L.; Yaron, J.; Lee, F.; Shi, Z.; Tian, Y.; Meldrum, D. R. *Angew. Chem., Int. Ed.* **2015**, *54*, 12053. (d) Yuan, L.; Wang, L.; Agrawalla, B. K.; Park, S.-J.; Zhu, H.; Sivaraman, B.; Peng, J.; Xu, Q.-H.; Chang, Y.-T. *J. Am. Chem. Soc.* **2015**, *137*, 5930.
- (14) A similar strategy has been used to unmask a methylene blue derivative in *E. coli*: Bae, J.; McNamara, L. E.; Nael, M. A.; Mahdi, F.; Doerksen, R. J.; Bidwell, G. L., III; Hammer, N. I.; Jo, S. *Chem. Commun.* **2015**, *51*, 12787.
- (15) Fluorochrome quinone–cyanine 7 system: (a) Karton-Lifshin, N.; Segal, E.; Omer, L.; Portnoy, M.; Satchi-Fainaro, R.; Shabat, D. *J. Am. Chem. Soc.* **2011**, *133*, 10960. (b) Redy-Keisar, O.; Kisin-Finfer, E.; Ferber, S.; Satchi-Fainaro, R.; Shabat, D. *Nat. Protoc.* **2014**, *9*, 27.
- (16) Danson, S.; Ward, T. H.; Butler, J.; Ranson, M. *Cancer Treat. Rev.* **2004**, *30*, 437.
- (17) While DT diaphorase is not involved in the activation of **2a–2c**, a recent report describes its use for another type of activation: Shin, S. S.; Lee, M.-G.; Verwilt, P.; Lee, J. H.; Chi, S.-G.; Kim, J. S. *Chem. Sci.* **2016**, DOI: 10.1039/c6sc02236g.
- (18) Koder, R. L.; Miller, A.-F. *Biochim. Biophys. Acta, Protein Struct. Mol. Enzymol.* **1998**, *1387*, 395.
- (19) Chevalier, A.; Zhang, Y.; Khodour, O. M.; Hecht, S. M. *Org. Lett.* **2016**, *18*, 2395.
- (20) Tzung, S.-P.; Kim, K. M.; Basanez, G.; Giedt, C. D.; Simon, J.; Zimmerberg, J.; Zhang, K. Y. J.; Hockenbery, D. M. *Nat. Cell Biol.* **2001**, *3*, 183.
- (21) Huang, L.-S.; Cobessi, D.; Tung, E. Y.; Berry, E. A. *J. Mol. Biol.* **2005**, *351*, 573.